Low-energy electron beam sterilization of solid alginate and chitosan, and their polyelectrolyte complexes

Maylis Farno, Camille Lamarche, Christophe Tenailleau, Sandrine Cavalié, Benjamin Duployer, Daniel Cussac, Angelo Parini, Brigitte Sallerin, Sophie Girod Fullana

Low-energy electron beam sterilization of solid alginate and chitosan, and their polyelectrolyte complexes

Maylis Farno[1,4], Camille Lamarche[2], Christophe Tenailleau[3], Sandrine Cavalié[1], Benjamin Duployer[3], Daniel Cussac[4], Angelo Parini[4], Brigitte Sallerin[4*] and Sophie Girod Fullana[1*]

[1] Université Paul Sabatier, CIRIMAT Institut Carnot Chimie Balard CIRIMAT, Faculté de Pharmacie, Toulouse, France

[2] ITHPP Alcen, Thégra, France

[3] Université Paul Sabatier, CIRIMAT Institut Carnot Chimie Balard CIRIMAT, UPS, Toulouse, France

[4] Université Paul Sabatier, I2MC, Toulouse, France

[*] these authors equally contributed to this work

Graphical abstract

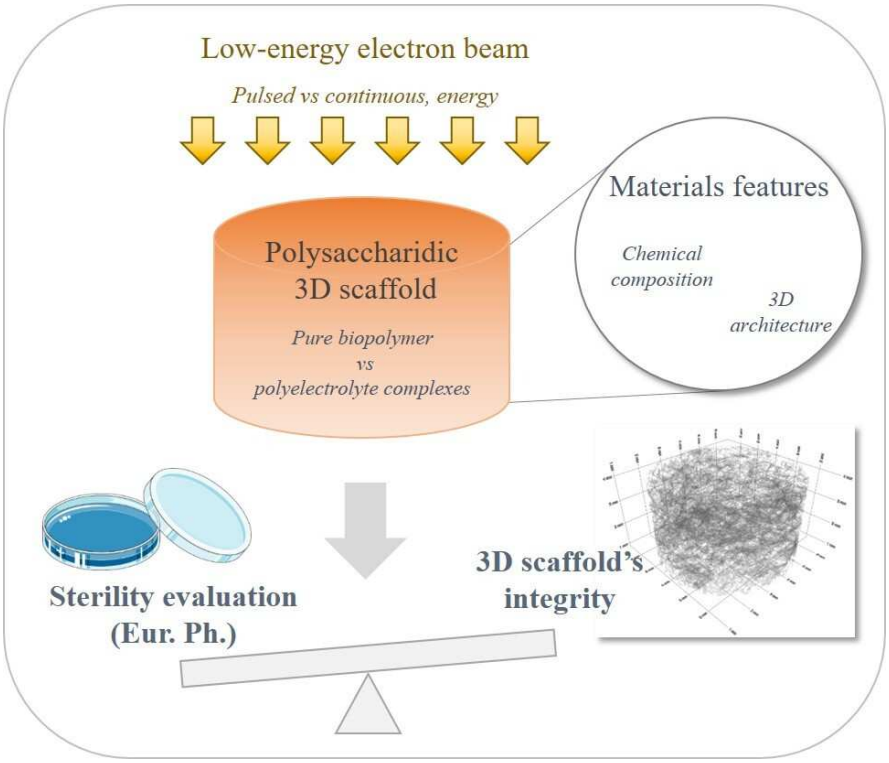

Highlights

- *Low-energy electron beams are valuable sterilization techniques for porous polysaccharidic networks*
- *Continuous beam irradiation lead to less depolymerization of alginate or chitosan alone*
- *PEC formation has a protective effect against degradation under irradiation*
- *Optimal settings of pulsed irradiation were found to sterilize PEC scaffolds*
- *Low-dose (<25 kGy) may be sufficient to sterilize 3D architectured polysaccharidic materials*

Key-words: *low-energy electron beams, sterilization, polysaccharides, alginate, chitosan, polyelectrolyte complexes, scaffolds*

Abstract

Polysaccharidic scaffolds hold great hope in regenerative medicine, however their sterilization still remains challenging since conventional methods are deleterious. Recently, electron beams (EB) have raised interest as emerging sterilization techniques. In this context, the aim of this work was to study the impact of EB irradiations on polysaccharidic macroporous scaffolds. The effects of continuous and pulsed low energy EB were examined on polysaccharidic or on polyelectrolyte complexes (PEC) scaffolds by SEC-MALLS, FTIR and EPR. Then the scaffolds' physicochemical properties: swelling, architecture and compressive modulus were investigated. Finally, sterility and in vitro biocompatibility of irradiated scaffolds were evaluated to validate the effectiveness of our approach. Continuous beam irradiations appear less deleterious on alginate and chitosan chains, but the use of a pulsed beam limits the time of irradiation and better preserve the architecture of PEC scaffolds. This work paves the way for low energy EB tailor-made sterilization of sensitive porous scaffolds.

1. ***Introduction***

During the past decades, polysaccharides-based scaffolds have been widely investigated in tissue engineering. The structural similarity of their network with the human extracellular matrix gives them the advantage of being highly biocompatible (Dai et al., 2016), with a good biodegradability (Shelke, James, Laurencin, & Kumbar, 2014). In this domain, alginate and chitosan are particularly of interest (Catoira, Fusaro, Di Francesco, Ramella, & Boccafoschi, 2019; Jose, Shalumon, & Chen, 2019). Their functional groups, carboxyl (-COOH) and amine (-NH2) respectively, allow ionic gelation, functionalization (to enhance solubility or promote cell adhesion) and their combination as polyelectrolyte complexes of opposite charges (PECs) (Croisier & Jérôme, 2013; Lee & Mooney, 2012; Sæther, Holme, Maurstad, Smidsrød, & Stokke, 2008; J. Sun & Tan, 2013; Xu et al., 2017). This last possibility improves their network mechanical properties (Li, Ramay, Hauch, Xiao, & Zhang, 2005) while maintaining their biocompatibility (Meka et al., 2017; Wang, Khor, Wee, & Lim, 2002).

Alginate-chitosan PECs formation may differ upon biopolymers characteristics (molecular weight, density of charges, degree of ionization, distribution of ionic groups) and conditions in which the polymers are brought together (concentration of polyelectrolytes, mixing ratio, order of reacting polyelectrolytes, pH of reaction medium, temperature, optional drying process, etc..), leading to multilayers, micro- or nano-particles or bulks (hydrogels, sponges, cryogels, aerogels..) (Luo & Wang, 2014) with potential applications in drug delivery and bone, cartilage, heart, or skin repair (Deka, Deka, Moni, Kumar, & Kumar, 2016; Florczyk et al., 2013; Kuznetsova, Andryukov, Besednova, Zaporozhets, & Kalinin, 2020; Li et al., 2005; Reed & Wu, 2015).
Our team developed some alginate-chitosan PEC sponges formulations, and demonstrated their interest as macroporous 3D-scaffolds for soft cell therapy purposes. These scaffolds exhibit controlled porosity and mechanical properties allowing in-depth cell seeding, optimization of mesenchymal stem cells (MSCs) survival and beneficial modification of their secretion profiles (Bushkalova et al., 2019; Ceccaldi et al., 2014). It is widely acknowledged that scaffold 3D architecture and seeded cells' fate can be correlated (Gómez, Vlad, López, & Fernández, 2016; Pennesi, Scaglione, Giannoni, & Quarto, 2011; Santos, Hernández, Pedraz, & Orive, 2012), thus finding an efficient sterilization technique preserving 3D scaffolds physicochemical features is a current challenge, all the more difficult to achieve when the material is of low density.

In this domain there is no gold standard, each method having its own advantages and drawbacks. Due to their organic nature, polysaccharides-based scaffolds may be exposed during sterilization to chemical and physical alterations as they share structural features with the vital components of pathogens (Munarin, Bozzini, Visai, Tanzi, & Petrini, 2013). These macromolecules tend to degrade when exposed to conventional sterilizing methods such as autoclaving or dry heating sterilization (França et al., 2013; Hu et al., 2014; Leo, Mcloughlin, & Malone, 1990; Rao & Sharma, 1995; San Juan et al., 2012; Vandenbossche, 1993). Other chemical treatments can be considered such as ethylene oxide or hydrogen peroxide exposition. However, besides their hazardous nature for users, they result in the formation of toxic by-products that can remain in the scaffold (Mendes, Brandão, & Da Silva, 2004; Rosiak, Ulanski, Kucharska, Dutkiewicz, & Judkiewizc, 1992). Ionizing radiations appear more environment-friendly; among them, gamma rays and beta radiations, *i.e.* electron beams, are the most frequently used for sterilization purposes of medical devices.

Gamma rays are photons emitted from the deexcitation of an atom (commonly ^{60}Co) while beta radiations involve particles, electrons, whose ability of penetration in matter is lower. Gamma rays are high-energy radiation, respectively 1.17 and 1.33 MeV, while electron beams can range from 200 keV to 10 MeV depending on the type of device. The inactivation of microorganisms following ionizing radiation has been thoroughly studied (Lamarche & Demol, 2018; Tallentire, Miller, & Helt-hansen, 2010; Zhu et al., 2008). Up to now both these radiations were mainly used for polysaccharides treatment to obtain oligosaccharides of low molecular weights with enhanced properties such as antioxidant, antibacterial or plant growth promoter (Feng, Du, Li, Hu, & Kennedy, 2008; Hien et al., 2000; Kume, Nagasawa, & Yoshii, 2002; Matsuhashi & Kume, 1997; Sen & Atik, 2012; Yoksan, Akashi, Miyata, & Chirachanchai, 2004). Many of these studies gave a great understanding of the mechanisms of ionizing radiations effects on polysaccharides. The degradative chemistry of irradiation on organic molecules is well described and consists in free radical initiation, propagation and termination events (Ciesla, 2017; Del Mastro, 2016; Gueven, 2004; Lim, Khor, & Koo, 1998; Yoksan et al., 2004). Most frequently ionizing radiations lead to biopolymer degradation through depolymerization mechanisms (Aliste, Vieira, & Del Mastro, 2000; Leo et al., 1990; Nagasawa, Mitomo, Yoshii, & Kume, 2000; Sen, Rendevski, Akkas-Kavaklı, & Sepehrianazar, 2010; Wasikiewicz, Yoshii, Nagasawa, Wach, & Mitomo, 2005; Wenwei, Xiaoguang, Li, Yuefang, & Jiazhen, 1993). Besides materials characteristics (chemical nature, solid state or in solution, thickness, density), ionizing radiation consequences depend on extrinsic parameters such as environmental conditions (temperature, oxygen or anoxic conditions, moisture content) and radiation parameters (energy, dose and dose-rate) (Chmielewski et al., 2007; Ciesla, 2017; Del Mastro, 2016; Lim et al., 1998; Yoksan et al., 2004). Thanks to its low penetration and high dose-rate, electron beam was first developed for material surface treatment but could easily be diverted for effective sterilization of thin and low-density macroporous materials without compromising their integrity. However much less is known about the sterilization of polysaccharides with electron beam: to our knowledge a scarce number of studies deal with alginate and chitosan beta sterilization (Gryczka et al., 2009; Silva, Elvira, Mano, Roma, & Reis, 2004) and none deals with their PECs. Thus, low energy electron beam could be a valuable sterilization technique for macroporous polysaccharidic scaffolds; the validation of this hypothesis is the purpose of this study.

In this work, an attempt has been made to compare continuous and pulsed low energy electron beam effects on the chemical properties of alginate, chitosan and their PECs, and on the physicochemical properties of alginate-chitosan PEC scaffolds, as well as their overall microbiocidal effectiveness. To that end, alginate or chitosan references scaffolds and PEC scaffolds have been irradiated with 300 keV continuous electron beam (CB) or with 280 keV or 430 keV pulsed electron beam (PB). First,

size exclusion chromatography (SEC), Attenuated Total Reflectance Fourier Transform InfraRed spectroscopy (ATR-FTIR) and Electron Paramagnetic Resonance (EPR) were achieved with the intention to unveil underlying chemical degradation mechanisms. Then, the effects of radiation sterilization on alginate-chitosan PEC scaffold' performances (swelling behavior, architecture and compressive mechanical properties) were evaluated. Finally, sterility assays according to European Pharmacopeia and *in vitro* biocompatibility tests were performed to determine if a sterilization at low dose is possible without altering the biomaterial's biocompatibility.

2. ***Materials and methods***

2.1. Materials

Sodium alginate medium viscosity (reference A-2033, batch 051M0054V), chitosan medium molecular weight (reference 448877, batch STBF8484V), HEPES sodium salt, acetic acid, EDTA, L-glutamine, fetal bovine serum (FBS), as well as antibiotics penicillin-streptomycin, were purchased from Sigma-Aldrich, France. Complete medium for cell culture was prepared by supplementing the Dulbecco's Modified Eagle's medium glutamax (reference 31966-021; ThermoFisher, France) and macrophage-colony stimulating factor (M-CSF) was purchased from Peprotech, France.Calcium chloride dihydrate ($CaCl_2 \cdot 2H_2O$), sodium chloride (NaCl) and sodium hydroxide (NaOH) were supplied from VWR. Sterile water was purchased from Cooper (France).

2.2. Polysaccharides characterization

Polysaccharides molecular weights were determined with size exclusion chromatography. The G/M units ratio of alginate was estimated by 1H NMR (Nuclear Magnetic Resonance) spectroscopy (Vilén, Klinger, & Sandström, 2011) to M/G= 2.1. The deacetylation degree (DD) of chitosan was estimated to be 75% by solid 13C NMR (Heux, Brugnerotto, Desbrières, Versali, & Rinaudo, 2000).

2.3. Preparation of Alginate/Chitosan macroporous 3D scaffolds

Three-dimensional alginate/chitosan PEC scaffolds containing alginate/chitosan weight ratio of 40/60 were prepared as reported previously (Bushkalova et al., 2019; Ceccaldi et al., 2014). Briefly, PEC scaffold were obtained by a combination of freeze-drying and gelation with $CaCl_2$ 0.1M. Final polymer concentrations in 40/60 PEC were respectively 1,5% w/w for alginate and 2,25% w/w for chitosan. Scaffolds made of alginate (ratio 100/0) or chitosan (ratio 0/100) 1.5% w/w were used as references. The final dimensions of 40/60 PEC scaffolds, used in all experiments, were 10 mm diameter × 5 mm thickness.

2.4. Low energy electron-beam treatments and dosimetry

Electron beam treatment was performed by two distinct low energy electron beam facilities in this study. The "continuous E-beam" (CB) equipment from COMET group (Flamatt, Switzerland) was used for continuous electron beam whereas the "Pulsed E-beam" (PB) equipment from ITHPP (Thégra, France) was used for pulsed radiation. Table 1 summarizes each generator features:

	CB	PB
Energy	300 keV	280 keV or 430 keV
Max beam current	from 1 to 15 mA	7 kA
Max dose-rate	10^5 kGy/s	10^{12} kGy/s
Pulse repetition frequency	-	5-100 Hz
Distance from extraction window	2 cm	2 cm

Table 1 - Continuous and pulsed generator features

Concerning the PB generator, in this study two different energies were studied 280 keV and 430 keV, with a pulse duration of 10 and 12 ns, respectively. Scaffolds were sealed into Stericlin® pouches as a sterile barrier packaging system, and were irradiated in order to reach 2.5, 5 and 25 kGy minimum absorbed doses at the bottom of the scaffold. Dose measurements were achieved by placing radiochromic dosimeters (Dosimetryfoil 20 µm (Crosslinking®)) below samples and inside the pouches. Directly after irradiation radiochromic films were incubated at 37°C for 15 minutes and passed through the "dose-reader DR 020" (Electron crosslinking AB, Sweden) to know the absorbed dose.

2.5. Chemical study

2.5.1. Size exclusion chromatography (SEC)

Experimental conditions for alginate and chitosan scaffolds dissolution and processing for SEC are resumed in Table 2. After scaffold dissolution, solutions were filtered through 0.45 µm nylon filter membrane. The detection was operated by a differential refractometer (Shodex RI-101) and a 18 angles static light scattering detector (MALLS Wyatt Dawn Heleos, laser = 658 nm; Wyatt Technology, USA) and a 254 nm UV detector (Varian, Australia). Data were analyzed with ASTRA VI software (Wyatt Technology, USA).

	Alginate	Chitosan
Dissolution buffer	50 mM EDTA	1M CH_3COOH (24h) + 0.2 M CH_3COOH / 0.15 M $NH_4CH_3CO_2$
Mobile phase	0.1 M $NaNO_3$ / 0.1g/L NaN_3	0.1M CH_3COONa / 0.1 M CH_3COOH
Flow rate	1 mL/min	0,8 mL/min
Injection volume	50 µL	50 µL
Columns	Shodex columns : 805, 804 and 802.5 (Showa Denko, Japan)	TSK gl PWXL-CP cationic columns : G5000 and G3000 (Tosoh, Japan)
dn/dc value	0.150 mL/g	0.192 mL/g

Table 2 - Size exclusion chromatography processing parameters for alginate and chitosan elution

2.5.2. Attenuated Total Reflectance Fourier Transform Infrared Spectroscopy (ATR-FTIR)

ATR-FTIR spectra of 3D scaffolds in solid state were recorded using a Nicolet iS50 Spectrometer (Thermo Fisher Scientific, Waltham, MA) in monoreflection with an ATR Crystal diamond, with a 2 cm^{-1} resolution over 64 scans in the range from 4000 to 400 cm^{-1}. The spectra baselines were normalized using Origin software (OriginLab Corporation, Northampton, MA, USA). For each scaffold spectra were analyzed for peak intensity changes with respect to reference band within the same spectra.

2.5.3. Electron paramagnetic resonance (EPR)

EPR experiments were acquired in X-band with a high-sensitivity cavity at room temperature, using a Bruker Elexsys with the following settings: power of 1 mW and a modulation of 1G. An angular dependence was observed: the spectra provided are the sum of the 8 spectra obtained by rotation of 45° with respect to the field.

2.6. Physicochemical characterization

2.6.1. Swelling

The swelling behaviors of irradiated scaffolds and their non-treated (NT) counterparts was studied at room temperature by measuring scaffolds' weight in a dry (W_{dry}) and in a wet (W_{wet}) state using an electronic balance (precision d=0.0001 g) as previously described (Bushkalova et al., 2019). The swelling ratio of each scaffold was calculated using the following formula: swelling ratio (%) = $[(W_{wet} - W_{dry})/ W_{dry}] \times 100$.

2.6.2. Scanning electron microscopy

Irradiated and NT scaffolds were coated under vacuum with 10 nm platinum alloy. Images were acquired with an electron microscope Quanta™ 250 FEG (FEI, USA) at an accelerating voltage of 5 kV. Both the irradiated surface and cross-section of each sample were examined at magnification 20 and 75 times.

2.6.3. Computed X-ray Micro-tomography (Micro-CT)

The micro-CT study of samples was carried out on Phoenix Nanotom180 (GE Sensing, Germany) using the following parameters: 60 kV voltage, 240 µA current, no filter material, 0.25° rotation step, 5 frames as frame averaging, 1440 tomographic projections over a 360°scan angle, 750 ms exposure time. A binning 1×1 was applied for the slices reconstruction and the resulting voxel size was 11.5 μm^3. Three-dimensional virtual models of scaffolds were obtained using VG StudioMAX 2.1. A region of interest (ROI) was drawn within the reconstructed volume and a threshold was defined to identify the polymeric phase. Then, a morphometric analysis of the ROI was performed to obtain the total porosity and void interconnectivity. Scaffold's pore walls thickness were analyzed on the basis of 2D X-ray tomographic slices using ImageJ (NIH, USA). ImageJ tool called "local thickness" was applied on cross-sections defined ROI, and subsequent color gradient allowed us to visualize polymeric thickness differences. Afterwards an ImageJ macro was developed to quantify relative

proportions of thick polymeric walls across scaffolds' depth through pixel quantification. For each condition, at least 30 slices were assessed, each slice corresponding to a 100 µm increment.

2.6.4.Mechanical properties under compression

Mechanical behavior of irradiated and NT scaffolds was evaluated by three successive uniaxial compression tests (TA-XT2 Texture Analyzer, Stable Microsystems, UK) in a hydrated state, according to a protocol already described (Ceccaldi et al., 2014). Prior to mechanical testing, the scaffolds were immersed in Milli-Q water for 24 hours at room temperature. The apparatus consisted of a mobile probe (1256.6 mm²) moving vertically up and down at a constant and predefined velocity (0.5 $mm.s^{-1}$) with a strain target of 50%. The stress area (mm²) of each scaffold and the force $F_{strain\%}$ (N) were collected. The secant moduli $E_{50\%}$ (kPa) were calculated from at least five independent observations as the slope of a line connecting the point of zero strain to a point at a 50% deformation.

2.7. Biological evaluation

2.7.1.Bioburden determination and sterility assay

Bioburden determination and sterility evaluation after irradiation were performed according to European standards, respectively ISO 11737-1 and ISO 11737-2. Initial bioburden of 3D scaffolds and bulk polymers were determined. Prior to sterility assays, scaffolds ability to allow microorganism growth was checked. Sterility assay of 40/60 PEC scaffolds was performed by incubating 5 pooled-samples in trypcase-soya broth (for aerobic bacteria) and 5 pooled-samples in thioglycolate broth with rezasurin (for anaerobic bacteria) as recommended in European Pharmacopeia (Ph. Eur. 2.6.1, 2008). Broth were respectively incubated at 22.5 ± 2.5 °C and 32.5 ± 2.5 °C, and were checked regularly for up to 14 days. If not stated otherwise all experiments were performed in triplicates (3 replicates of 5 pooled-samples for each broth).

2.7.2.In vitro biocompatibility after irradiation

For in vitro biocompatibility evaluation, primary bone-marrow derived murine macrophages were used. Briefly, cells were isolated from femurs and tibiae of C57BL/6 mice, red blood cells were then lysed with ACK (Ammonium-Chloride-Potassium) lysis buffer. BMDM were selected by adhesion to petri dishes after 4 days of differentiation in DMEM glutamax medium supplemented with 10% FBS, 1% penicillin-streptomycin, 1% L-glutamine and 30 ng/mL M-CSF. Cell seeding on scaffolds was performed according to previously described protocol (Bushkalova et al., 2019). After 24 hours Live/Dead assays were performed on seeded scaffolds using the Viability/Cytotoxicity Assay kit (FluoProbes®, Interchim, France). Staining solution were concentrated with 2 µM ethidium homodimer-3 (necrotic marker measuring nucleus membrane integrity) and 1 µM calcein AM (viability marker measuring the intracellular esterase activity). Confocal microscopy was achieved (Zeiss LSM780) by exciting samples with a 488 nm Argon laser and with a 543 nm helium–neon laser, and using 10X objective. Then three-dimensional reconstructions were generated using IMARIS software (Bitplane) from microscopic images where the green and red channels were merged.

2.8. Statistical analysis

Data in the figures are given as mean ± standard error of the mean (SEM). Statistical significances were determined using Graph Pad Prism software by unpaired t-tests if only two groups were in the study or by two-way analysis of variance (ANOVA) with Tukey post-tests for multiple comparisons with more than two groups (GraphPad Prism 6, version 6.01). Differences between the groups were considered as statistically significant at the level of $p < 0.05$ and marked with asterisks (*; **; *** = $p < 0.05$; 0.01; 0.001).

3. *Results and discussion*

3.1. Dose distribution across 3D scaffolds

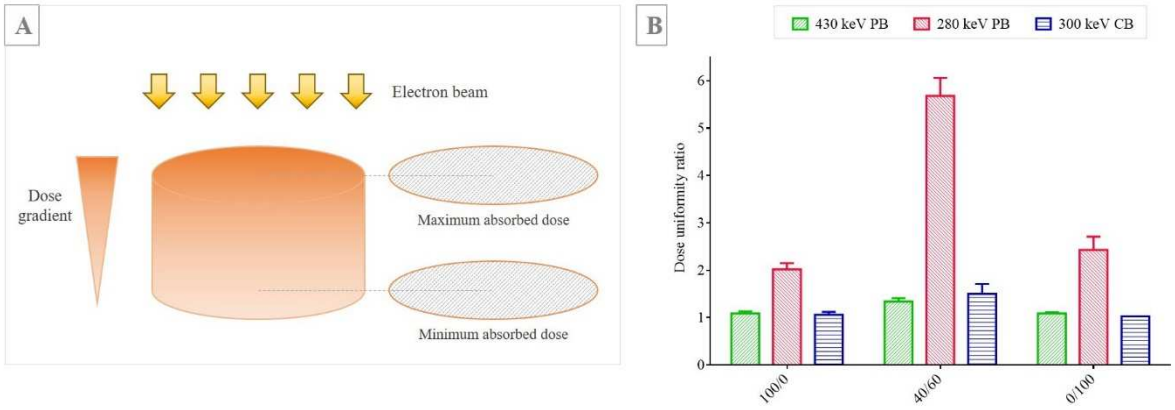

Figure 1 - Dose distribution through PEC scaffolds. A) Diagram showing maximum and minimum dose localization. B) Dose uniformity ratios of 40/60 PEC scaffolds and references scaffolds (100/0 and 0/100) according to the electron beam treatment applied

In order to compare the effect of pulsed versus continuous electron beam, we decided in a first approach to work at similar energy level (i.e. to compare 280 keV PB *vs* 300 keV CB) with equal minimum absorbed dose, assuming that the minimum absorbed dose was reached at the bottom of PEC scaffolds (Figure 1). Dose setting was established as 2.5, 5 and 25 kGy, the latter being the sterilizing dose required in European standards. Although 25 kGy effect on PEC is to date still unknown, it is likely to be detrimental so we decided to test lower doses such as 2.5 and 5 kGy and to evaluate their sterilizing properties. Dose uniformity ratios (DUR) were calculated as the ratio of maximum and minimum absorbed doses. Whatever the irradiation treatment, PB provides a less homogenous dose deposition. This heterogeneity is more pronounced in the case PEC scaffolds (Figure 1), because of PEC scaffolds' higher density due to stronger interchain interactions. As a consequence, we decided to include in our study a third condition corresponding to a higher PB electron energy of 430 keV, for a similar dose uniformity with 300 keV CB. Indeed, energy is known to be a key factor concerning the DUR of an irradiated product (Helt-Hansen et al., 2010; Lambert & Martin, 2013). DUR differences between PB and CB at a same level of energy is a consequence of voltage signal's shape, which is a bell shape in the case of PB generator. Consequently, a non-negligible part of electrons have a lower energy than 280 or 430 keV (Lamarche, 2019). For the 430 keV generator, the mean energy of electron beam is 302 keV, a value almost similar to that of CB generator.

This work is a comparative study of pulsed and continuous electron beam at similar energy levels (280 keV PB and 300 keV CB) or at similar DUR ratios (430 keV PB and 300 keV CB). We aimed at evaluating electron beam irradiation effect on both polysaccharides chemical properties and scaffolds 3D architecture, which are crucial for biomaterials biocompatibility. Due to technical limitations, PEC

chemical changes were not pursued as thoroughly as for pure biopolymers, but were assessed by indirect methods.

3.2. Study of chemical changes after irradiation

On the contrary of the well-studied degradation effects of gamma irradiation on polysaccharides, and especially on alginate and chitosan, low-energy beta irradiation chemical effects are yet to be thoroughly evaluated. Alginate and chitosan were irradiated in the solid state, which is known to be less sensitive to irradiation effects than the liquid state (Hien et al., 2000; Kume et al., 2002; Nagasawa et al., 2000; San Juan et al., 2012; Wasikiewicz et al., 2005). Biopolymer's sensitivity to irradiation depends on some intrinsic properties of starting material such as the M/G ratio of alginate and degree of deacetylation (DDA) for chitosan, although those values are not expected to change in themselves upon irradiation. Sen and coworkers have shown that alginate degradation increased with a higher mannuronate content (Sen et al., 2010). Others have shown that even if irradiation does not induce any changes with regards to DDA (Lim et al., 1998; Zainol, Akil, & Mastor, 2009), it is mostly effective on acetylated parts of chitosan, implying a higher degradation susceptibility with higher DDA (Taskin, Canisag, & Sen, 2014; Wenwei et al., 1993).

The weight average molecular weight Mw and the polydispersity index Đ of the polymers constituting the scaffolds were evaluated by SEC-MALLS (Figure 2). This technique was not applicable on PEC scaffolds as PEC can hardly be dissociated.

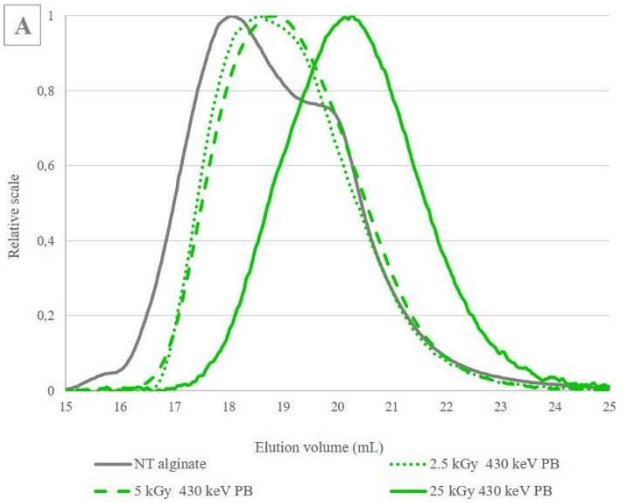

B

		Mw	Đ
	NT polymer	193 100	1,5
2,5 kGy	430 keV PB	137 000	1,7
	280 keV PB	141 900	1,5
	300 keV CB	153 600	1,65
5 kGy	430 keV PB	125 600	1,6
	280 keV PB	94 380	1,6
	300 keV CB	117 300	1,7
25 kGy	430 keV PB	48 530	1,5
	280 keV PB	64 280	2,4
	300 keV CB	61 220	1,75

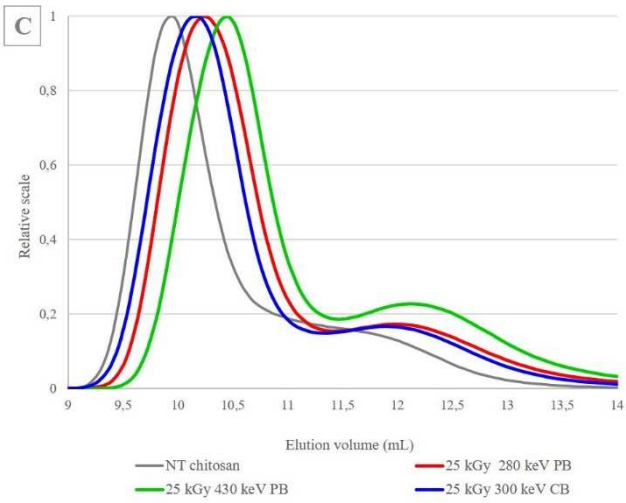

D

		Mw	Đ
	NT polymer	216 300	1,8
2,5 kGy	430 keV PB	95 070	1,5
	280 keV PB	182 300	1,8
	300 keV CB	224 900	2
5 kGy	430 keV PB	89 760	1,4
	280 keV PB	116 400	1,8
	300 keV CB	142 000	1,6
25 kGy	430 keV PB	60 400	1,6
	280 keV PB	72 100	1,7
	300 keV CB	101 800	1,7

Figure 2 - Irradiation impact on alginate and chitosan molecular weight. Graph A shows elution curves obtained with light scattering detector of 430 keV PB treated alginate references scaffolds (100/0) after different doses. Graph C shows elution curves of 25 kGy irradiated chitosan references scaffold (0/100) after different irradiation treatments. Tables B and D indicate the corresponding molecular weight values Mw and polydispersity D index D.

In the case of alginate, the Mw distribution evolves from slightly bimodal to monomodal after irradiation. In the case of chitosan it remains bimodal. Such bimodal shape is typical of chitosan samples (Thevarajah, Bulanadi, Wagner, Gaborieau, & Castignolles, 2016; Yanagisawa, Kato, Yoshida, & Isogai, 2006), and is related to high mass aggregates which were not taken into account for Mw determination. As expected, Mw decreases with increasing irradiation dose (Figure 2, Graph A). Whatever the irradiation technique, the effect of 2.5 kGy is limited for both polymers, whereas 25 kGy, which is the suggested sterilizing dose in norms (NF EN ISO 11137-2, 2006), appears clearly deleterious on Mw. Such a decrease testifies for main chain scission. By direct energy absorption, the main carbon chain depolymerizes as a consequence of glycosidic bonds cleavages. Both polymers appeared depolymerized upon irradiation, however chitosan chains appeared more sensitive than alginate chains to an energy increase from 280 keV to 430 keV (when irradiated at 2.5kGy chitosan depolymerizes 4-fold more at 430 keV than 280 keV). Some differences are observable according to irradiation treatment (Figure 2, Graph C), especially at 25 kGy: 300 keV CB seems to induce less polymer chain degradation than PB. This could be due to lower beam current associated with the CB

generator, which implies a lower electron flow and thus leads to less damaging effect (Table 1). An irradiation dose of 2.5 kGy do not prevent alginate nor chitosan polymers from scission events but they are limited, particularly in the case of CB irradiation.

The study of irradiation effects on alginate and chitosan scaffolds was supplemented by FTIR analyses to assess any functionality changes of alginate, chitosan or their PEC formation, caused by irradiation. ATR-FTIR spectroscopy was performed on 25 kGy irradiated scaffolds in order to identify at a surface level potential changes in functional groups or new bonds formation (Figure 3). For each biopolymer, the most representative signals were followed. Concerning alginate spectra (Figure 3), peaks at 3290 cm^{-1}, 1590 cm^{-1}, 1410 cm^{-1} and 1025 cm^{-1} can be respectively ascribed to hydroxyl O-H stretching, asymmetric and symmetric carboxylate salts COO^- stretching and finally glycosidic C-O-C bonds (Daemi & Barikani, 2012; Sartori, Finch, & Ralph, 1997; Yu, Cauchois, Schmitt, Louvet, & Six, 2017). For chitosan spectra (Figure 3, Graph B), the most representative peaks were at 3290 cm^{-1}, 1578 cm^{-1} and 1148 cm^{-1} which can be respectively attributed to hydroxyl, N-H bending from amine and amide II and finally C-O-C groups (Ji & Shi, 2013; Lawrie et al., 2007; Pawlak & Mucha, 2003). Relative peak intensity were calculated using carboxylate group and amine/amide group as references band for alginate and chitosan within each spectra as they are not supposed to change under irradiation (Wasikiewicz et al., 2005; Wenwei et al., 1993). Concerning chitosan spectra, an increase of hydroxyl groups, associated with a decrease of C-O-C groups, is in accordance with the hypothesized glycosidic bonds (C-O-C) cleavages, leading to hydroxyl group formation (Wenwei et al., 1993). In the case of alginate, differences between irradiated scaffolds at 25 kGy are more tenuous to detect and no new band appeared. PEC spectra (Figure 3, Graph C) are more similar to alginate ones but they display band shifts from 1590 cm^{-1} to 1595 cm^{-1} and 1410 cm^{-1} to 1414 cm^{-1}. These shifts have been attributed to an overlap of the amide signal of chitosan and alginate carboxylate groups, confirming polymers interaction (Lawrie et al., 2007; W. Sun et al., 2018) and thus PEC presence. No change in intensity of the peaks of PEC spectra was observed after irradiation treatments (Figure 3, Graph C); this suggests that PECs are not affected by beta irradiation, whatever the beam type and the energy tested in our study.

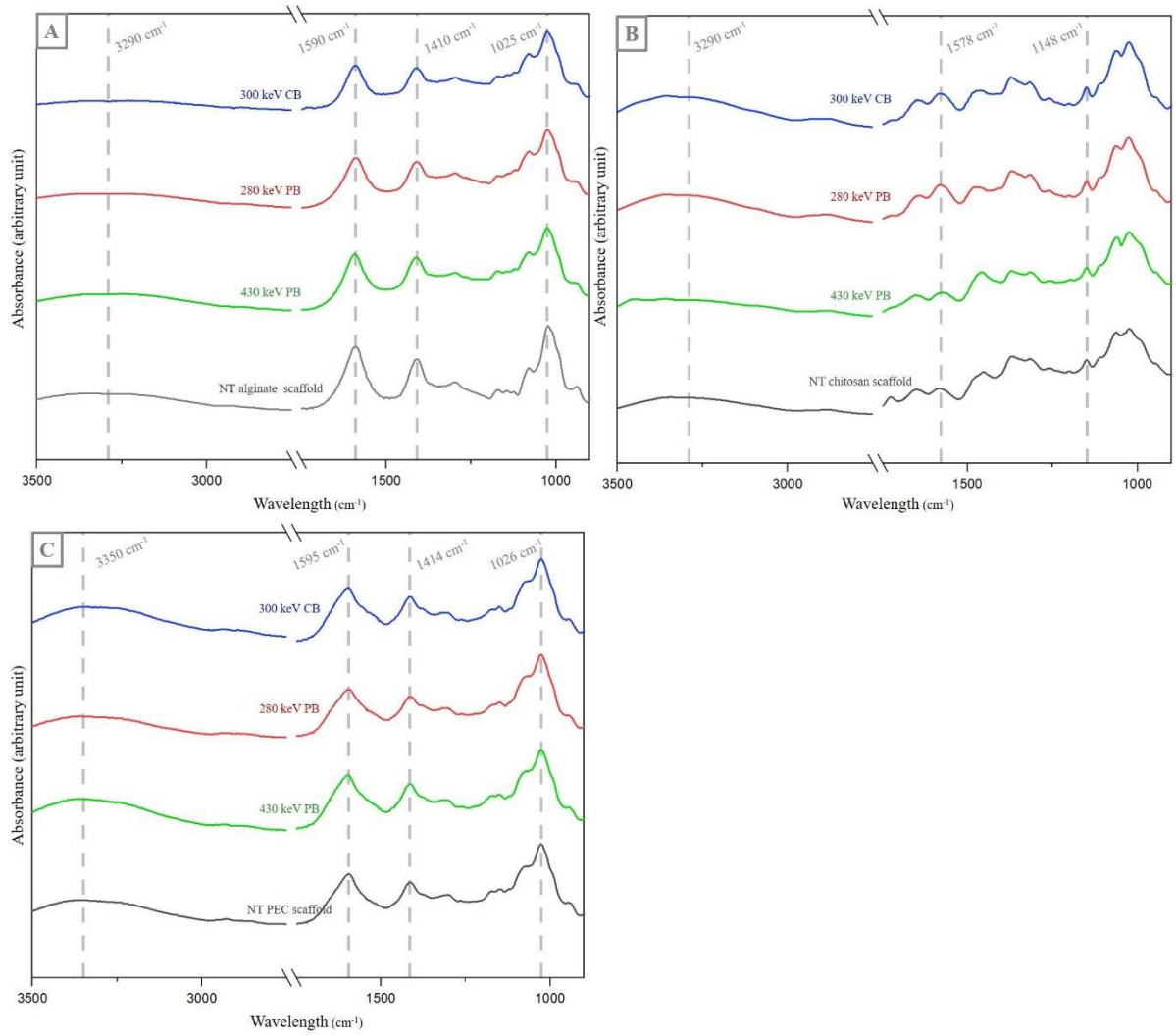

Figure 3 - FTIR analysis of non-irradiated and 25 kGy irradiated scaffolds. FTIR spectra with ATR reflection mode of alginate (Graph A), chitosan (Graph B) and PEC scaffolds (Graph C).

EPR is described as a useful tool to detect free radicals formation after irradiation of biodegradable polymers (Gryczka et al., 2009; Mäder, Domb, & Swartz, 1996). The presence of such radicals may cause cell oxidative stress, which could hence impact further scaffold biocompatibility and interest for regenerative applications. Because PB revealed a higher damaging effect on polysaccharides, we evaluated the amount of organic radicals in PEC scaffold over time after 280 keV and 430 keV PB irradiation by EPR. For both PB conditions, there is an obvious dissipation of such radicals (Figure 4). The presence of organic radicals confirms carbon backbone scission mechanism (Ershov, 1987; Rosiak et al., 1992). However, it is interesting to note that their presence remains negligible at 2.5 kGy, and moderate at 5 kGy whatever the PB energy tested. In both cases, the level of radicals goes back to normal within a week, with a RPE signal similar to the NT reference scaffolds. At higher irradiation energy (25 kGy), the presence of free radicals is significantly higher, even if after a week it appears considerably decreased.

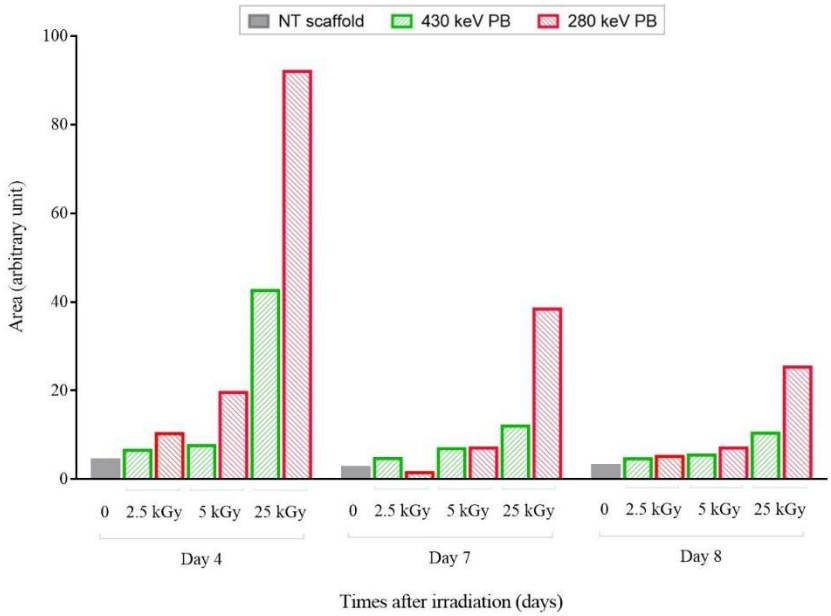

Figure 4 - Evolution of the amount of organic radicals present in PEC scaffolds at 4, 7 and 8 days after pulsed beam irradiation treatment.

FTIR and SEC results on pure polymer scaffolds show that both biopolymers depolymerize under low-energy electron beam irradiation as doses increase; this could have been limited by adapting the features of the starting polymers, i.e. with a lower M/G ratio for alginate or a lower DDA for chitosan. In this study, chitosan scaffolds seem to be more sensitive to irradiation-induced degradation than alginate ones. Whatever the type of electron beam, the lower the dose, the lower the deleterious effects. Concerning pure polymers, CB appears more adapted to scaffolds sterilization as its depolymerizing effects are lower than those observed at the tested PB doses. The low doses of 2.5 and 5 kGy clearly appear less deleterious than 25 kGy. Concerning the PEC scaffolds, they appear more resistant to irradiation thanks to their strong chain-to-chain interactions and consecutive higher density. In their case, both PB and EB seem applicable, particularly at low doses.

Anyway, a simple study on the chemical effects of electron beam irradiations on biopolymers is insufficient to predict the deleterious effects of these irradiations on 3D materials intended to be seeded with cells. Indeed, in this case, the specifications of the material go well beyond its simple composition: its retention in rehydration, its 3D architecture, its porosity, its mechanical resistance are all essential characteristics influencing the fate of cells at their contact. Therefore, a complete study of the effects of irradiation on this type of material must take into account the macroscopic effects of irradiations on 3D structures. With the aim to find radiosterilization operating conditions respecting scaffold's specifications, while ensuring its sterility, the main physico-chemical characteristics of irradiated PEC scaffolds were studied and compared to reference non irradiated scaffold.

3.3. Effect of various irradiation treatments on 3D scaffolds physicochemical properties

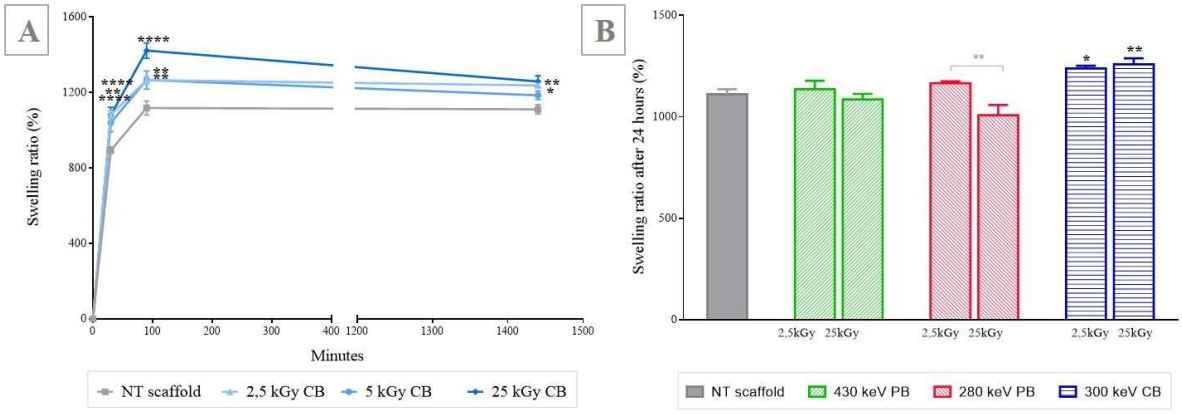

*Figure 5 - Swelling behavior of irradiated and non-irradiated 40-60 PEC scaffolds. Graph A shows continuous beam swelling kinetic, and graph B shows swelling ratio after 24 hours for all irradiation conditions. Five replicates were used for each condition (n=5; two-way ANOVA; *p<0.05; **p<0.01; **** p<0.0001; significant differences with NT scaffold and within the same irradiation treatment are respectively shown with black bold asterisks and grey asterisks)*

First, a particular attention was paid to scaffolds swelling properties, as stability under rehydration means that chemical bonds remain sufficient in number to ensure macroscopic cohesion. The swelling curves of all the scaffolds, irradiated or not, exhibited the same shape (Figure 5). In the first 30 minutes, scaffolds absorb 75% of total absorbed volume and reach a plateau within 4 hours, with for some samples a decrease in slope which can be attributed to sample sensitivity to successive handling. Water uptake was significantly higher after 300 keV CB treatment (Figure 5), suggesting a loosening of the scaffold network in this case. These differences in swelling ratio after a terminal sterilization treatment testify modification of the network architecture (Stoppel et al., 2013).

In order to gain insight on scaffolds architecture after irradiation, SEM images of 40-60 PEC scaffolds cross-sections (Figure 6) and surfaces (see supplementary data for surface SEM images) were acquired. All images displayed an interconnected macroporous structure which is mandatory for in-depth cell seeding, and therefore essential to preserve upon irradiation. At a 2.5 kGy dose no particular differences can be mentioned about scaffolds architecture. For doses higher than 2.5 kGy, pores walls seem more friable and the whole structure appears more fragile with increasing doses. Qualitatively, no differences can be pointed out between CB and PB.

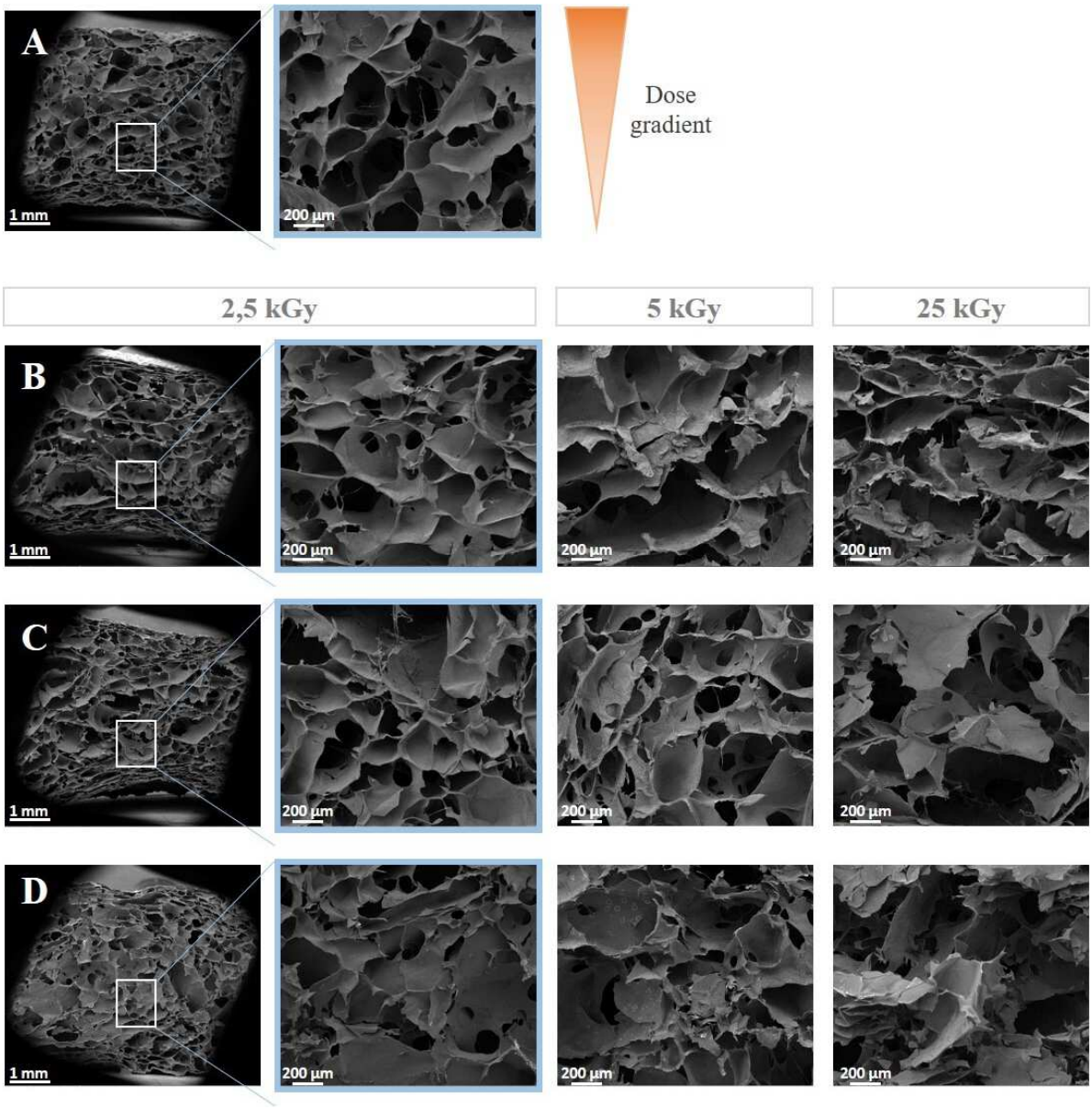

Figure 6 - Representative images of 40-60 PEC scaffold cross-section acquired by scanning electron microscopy (A) non irradiated scaffold (B) 430 keV pulsed beam (C) 280 keV pulsed beam and (D) 300 keV continuous beam (magnifications X20 and X75, corresponding scale bars are respectively 1 mm and 200 µm)

Scaffolds architecture analysis was expanded with micro-CT scans. From a qualitative point of view, scaffolds showed a similar airy foam structure before and after irradiation treatment (Figure 7, Graph A). Porosity quantification was estimated to 96% and confirmed a highly porous and entirely interconnected structure, allowing optimal cell seeding as previously demonstrated by our group (Bushkalova et al., 2019). Considering the higher DUR (Figure 1) observed when irradiating PEC scaffolds with PB at 280 keV, it seemed important to assess degradation degree depending on scaffold's depth or distance to the beam source. To that end, pore walls thickness was measured to study its distribution across scaffold's depth. Thicker walls might be related to PEC, whereas thinner ones might be imputable to single polymers network (alginate or chitosan). The limit of detection of thinner walls with thresholding didn't permit to study the latter, but was adapted for the former.

Graph B and C from Figure 7 shows 280 keV PB, 2.5 kGy, data as the irradiation treatment giving the highest DUR and likely to show a degradation gradient. No changes were observed across scaffolds' depth, confirming indirectly that PEC were not impacted by irradiation.

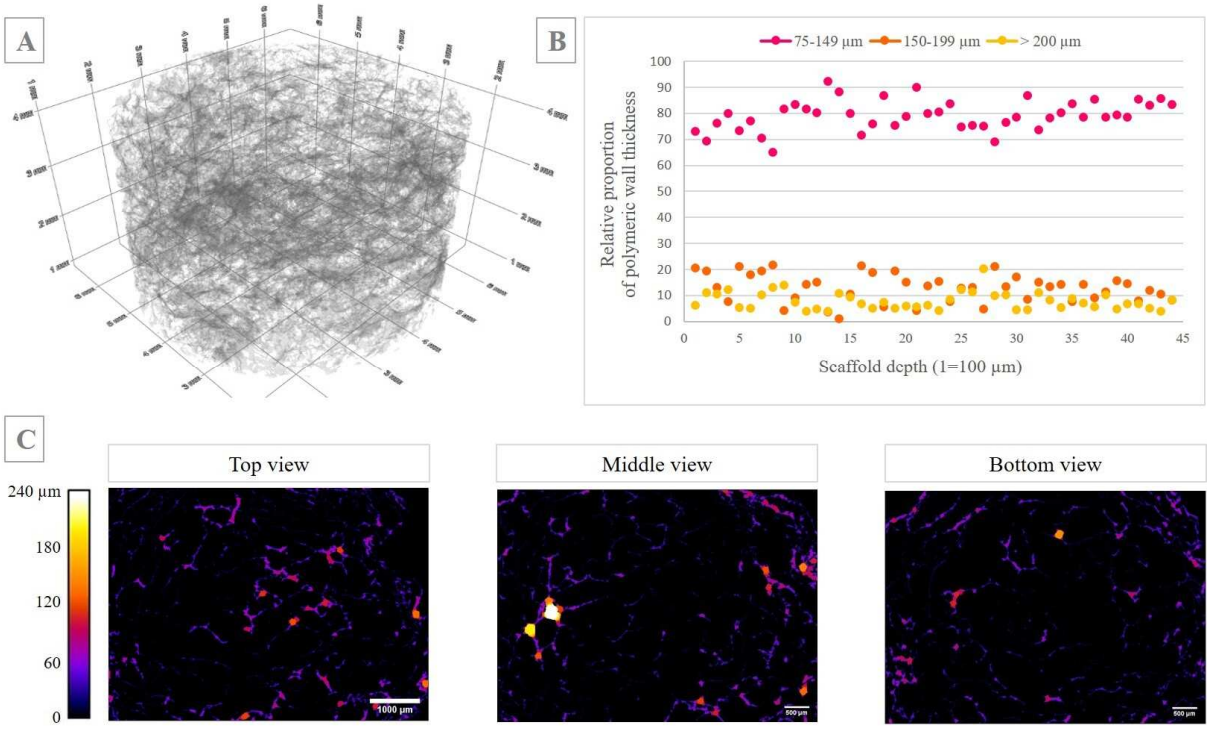

Figure 7 - Micro-CT analysis of 40-60 PEC scaffold. Volume reconstruction of 2.5 kGy irradiated 40-60 PEC scaffold with 280 keV PB (Image A). Relative proportions of polymeric wall thickness among walls thicker than 75 µm (Graph B) and corresponding cross sections ROI after ImageJ local thickness analysis (Image C).

Finally, compression tests give additional understanding on how scaffolds react to irradiation and how these modifications impact the scaffolds mechanical behavior. Overall compressive moduli increased with successive compression, meaning a stiffness increase due to water elimination during scaffolds compression. This behavior remained unchanged after irradiation (Figure 8, Graph B). First, PEC scaffolds showed a decrease of their mechanical resistance after irradiation (at least 28% and 37% decrease at 2.5 kGy for 280 keV PB and 300 keV CB, respectively) on their first compression (Figure 8, Graph A) but still fit in the range of magnitude of soft tissues elastic moduli (Guimarães, Gasperini, Marques, & Reis, 2020). However, 25 kGy is clearly detrimental for PEC scaffolds whatever the irradiation treatment. Finally, 430 keV PB treatment revealed only slight compressive moduli changes and offers the best scaffolds mechanical properties preservation. A major difference between continuous and pulsed electron beam technologies is the dose rate they offer (Chalise, Hotta, Matak, & Jaczynski, 2007; Lamarche, 2019). Electron beam technologies offer much higher dose rate than gamma radiations especially when electron beam is pulsed (Gotzmann et al., 2018; Silindir & Özer, 2009; Ziaie, Anvari, Ghaffari, & Borhani, 2005). Higher dose rate implies shorter treatment times and usually results in less damaging effect on the materials. This assumption is confirmed here as 430 keV PB irradiation is less damaging than 300 keV CB even if its energy is higher.

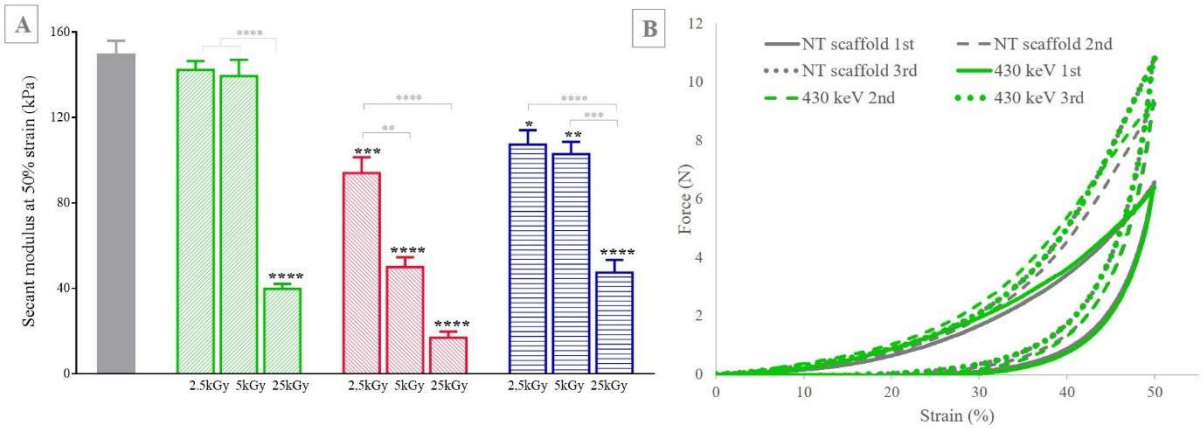

*Figure 8 – Secant modulus of irradiated and non-irradiated 40-60 PEC scaffolds measured at 50% compressive strain (Graph A). Graph B shows the force needed to reach 50% strain after three successive compression of NT and 2.5 kGy 430 keV irradiated scaffolds. Five replicates were used for each condition (n=5; two-way ANOVA; **p<0.001; **** p<0.0001; significant differences with NT scaffold and within the same irradiation treatment are respectively shown with black bold asterisks and grey asterisks).*

The results of this physico-chemical study on irradiated PEC scaffolds complete and confirm the results of the chemical study. Whatever the type of electron beam, the doses at 25kGy are deleterious for the scaffolds whose porous architecture appears weakened and mechanical properties strongly reduced, even if the scaffolds generally resist rehydration. PEC scaffolds were affected by irradiation on a dose-dependent way, but to an acceptable extent at low dose such as 2.5 kGy. While continuous beam appeared more suitable for scaffolds made of alginate or chitosan, the pulsed electron beam at low dose has given the best results for PEC scaffolds, with preserved rehydration, porous structure and wall thickness. Scaffolds' mechanical integrity was even preserved when irradiated with 430 keV PB. This can be explained by the higher dose rate and subsequently shorter treatment time permitted by pulsed beam compared to continuous beam, and by the better dose uniformity at 430 keV.

Critical comparison of the results obtained in this study with other electron beam sterilization/irradiation studies dealing with similar materials is quite challenging. To our knowledge, electron beam sterilization/irradiation of alginate has never been reported in the literature. Whereas several studies highlight chitosan depolymerization after electron beam irradiation, most of them where achieved at 10 MeV and concern chitosan under various physical conditions (Chmielewski et al., 2007; Gryczka et al., 2009; Matsuhashi & Kume, 1997; San Juan et al., 2012; Silva et al., 2004; Stößel et al., 2018). Thus, direct comparison of our results, obtained with alginate and/or chitosan in solid state, with other works is not self-evident since the starting carbohydrate polymers present different features (physical form, thickness and density if solid state) which impact their response to irradiation. However, our results are in accordance with other teams findings concerning the degradation mechanism of polysaccharides upon ionizing radiations.

3.4. Biological evaluation of sterilized scaffolds

Surprisingly, there are few studies in the literature that actually assess the sterility of materials after irradiation (Asasutjarit et al., 2017; Galante, Pinto, & Serro, 2017; Hartman, Nesbitt, Smith, & Nuessle, 1975; Hu et al., 2014; Rao & Sharma, 1995). In our case, sterility assessment was essential to validate irradiations at low doses. As specified in European standard 11137-2, sterilizing dose establishment can be obtained through two alternative methods to ensure a predetermined sterility assurance level (SAL). The most common method, called VDmax method, consists in the

substantiation of 15 or 25 kGy as sterilization dose. The other method relies on a dose setting to obtain a product-specific dose. The latter method was the one applied in this study because of the sensitivity of alginate and chitosan to high doses such as 15 or 25 kGy. Thus, bioburden determination is required and was obtained in accordance with 2.6.1 European Pharmacopeia chapter (Ph. Eur. 2.6.1, 2008). Bioburden is the result of microbial contributions from raw materials, manufacturing steps and product packaging. As Table 3 shows, bioburdens were very low whatever the scaffolds chemical composition, which permits the use of low doses for sterilization (Table 3).

At 2.5 kGy, only 280 keV PB irradiation ensured PEC scaffolds' sterility. It is likely that the high DUR in these conditions is responsible of this result. It allows to reach the sterilizing dose that is not reached at 430 keV PB and 300 keV CB, without exceeding the tolerance of the biomaterial as scaffolds' integrity over rehydration and porous architecture were preserved, with acceptable (although diminished) mechanical properties for soft tissue applications.

A

Alginate/chitosan ratio	Bioburden average quantification
Alginate 100/0	< 6 CFU / scaffold
PEC 40/60	< 6 CFU / scaffold
Chitosan 0/100	< 6 CFU / scaffold

B

PEC 40/60		Pulsed		Continuous
		430 keV	280 keV	300 keV
Minimum absorbed dose	2.5 kGy	-	+	-

Table 3 – Biological evaluation. Table A indicate bioburden determination according to alginate/chitosan ratio. Duplicates of 5-pooled samples were used. Table B shows sterility results in both aerobic and anaerobic conditions according to 2.6.1 European Pharmacopeia chapter. For each broth type, sterility assays was performed with three replicates (n=3) or a single replicate (n=1) of 5-pooled samples respectively for pulsed irradiation and continuous irradiation.

In this study, the feasibility of using low-energy pulsed electron beam for the sterilization of porous scaffolds of polysaccharidic nature was demonstrated (at 280 keV PB). Despite validated sterility assays, as recommended in European Pharmacopoeia, those conditions do not fulfill the requirement of the current European irradiation sterilization standards, since they do not address emerging techniques like low-energy irradiations. Other works also demonstrated the establishment of sterilizing doses for sensitive polysaccharides or complex medical devices at lower doses than required in the norms (Alcaraz et al., 2016; Farag Zaied, Mohamed Youssef, Desouky, & Salah El Dien, 2007). In the years to come, European standards will have to take into account the use of low-energy irradiation technologies able to answer to the sterilization needs of new materials such as porous polysaccharidic scaffolds. In that sense, the lack of standards for low-energy electron dosimetry has been underlined in recent study (Helt-Hansen et al., 2010); this observation can be extended to the sterilizing dose establishment after low-energy electron beam irradiation.

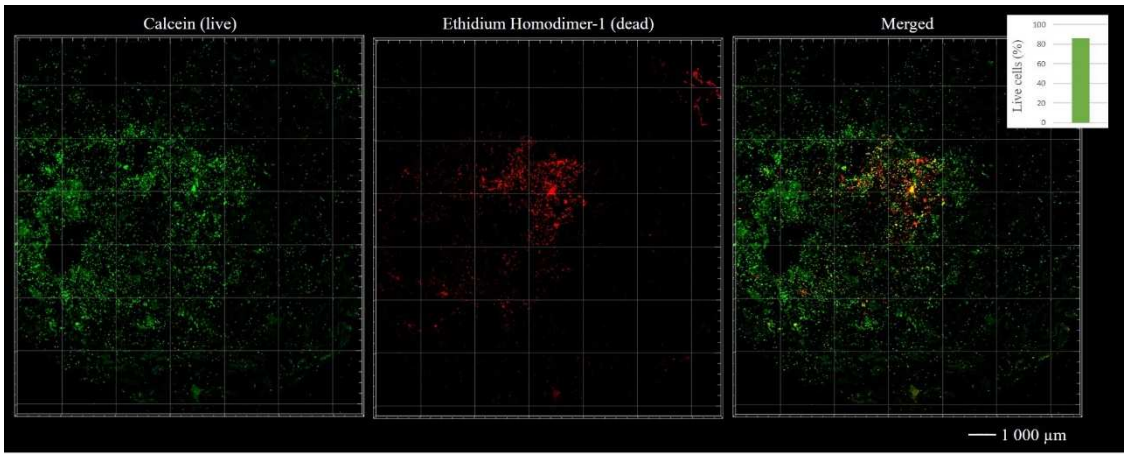

Figure 9 - 3D reconstruction of confocal microscopy images after Live/Dead staining of BMDM macrophages seeded 40-60 PEC scaffold after 2.5 kGy irradiation with 280 keV PB generator. Scale bar corresponds to 1000 µm.

In order to definitively validate the operating conditions for sterilization of PEC scaffolds, an in vitro biocompatibility study was carried out on sterilized scaffolds. Scaffolds were irradiated with 2.5 kGy PB with an energy of 280 keV, before BMDM seeding. After 24 hours, in vitro constructs were stained fluorescent viability markers which stain dead cells in red and live cells in green. Scaffolds were imaged in depth with a confocal microscope. Finally, 3D reconstructions were obtained (Figure 9) and cell viability was estimated to 86% (number of green cells over total number of green and red cells). As previously demonstrated with other cell types such as mesenchymal stem cells (Bushkalova et al., 2019; Ceccaldi et al., 2014), 40-60 PEC scaffolds biocompatibility was high and maintained even after low-energy electron beam sterilization.

4. Conclusions

To our knowledge, this is the first study concerning low-energy electron beam use for sterilization of polysaccharidic scaffolds, and more particularly those made of alginate, chitosan or their complexes. Sterilization of polysaccharides materials is still an unmet challenge for tissue engineering. Irradiation technologies remain very promising in that sense that they are environmentally friendly and do not produce toxic residues that could threaten scaffolds biocompatibility. In this work we have compared continuous and pulsed low-energy electron beam technologies and their impact on polysaccharides-based biomaterial properties for sterilization purposes. If irradiation-induced degradation cannot be denied on single alginate and chitosan polymers, it is highly limited when alginate and chitosan form polyelectrolyte complexes. An optimal sterilizing dose setting was found without compromising scaffolds properties when irradiated with 280 keV PB. This work paves the way for low-energy electron-beam sterilization of porous natural biopolymer materials. However low penetration ability limits the size of the constructs that can be sterilized and an adaptation of the beam energy is needed to achieve dose uniformity within the considered scaffold. In this way, European norms should consider low-energy irradiation suitability in the particular case of thin and low-dense materials such as 3D scaffolds developed for tissue engineering purposes.

Acknowledgments

This work was supported by Région Occitanie and INSERM grants. We are particularly grateful for the help provided by ITHPP Alcen (Thégra, France) for pulsed-beam irradiation treatments and helpful scientific discussions. We wish to thank E-beam technologies (COMET AG, Switzerland) for continuous beam irradiation service, Pascale Saint-Aguet from the "Plateforme Technologique pour la Caractérisation de Matériaux Polymères" (Technopolym platform, Toulouse, France) for SEC measurements, Olivier Marsan for ATR FTIR technical support (CIRIMAT), Lionel Rechignat for EPR measurements (LCC, Toulouse), the "Centre de Microscopie Electronique Appliquée à la Biologie" (CMEAB platform, Toulouse, France) for SEM facility, the Cellular Imaging Facility (T.R.I. Genotoul Plateform, Toulouse, France) for confocal facility, the FERMAT federation for X-ray tomography facility, and the FONDEREPHAR foundation for microbiological assay (Toulouse, France).

References

Alcaraz, J. P., Ichi-Ribault, S. El, Cortella, L., Guimier-Pingault, C., Zebda, A., Cinquin, P., & Martin, D. K. (2016). La biopile enzymatique à glucose/oxygène : Quelques nuances de Grays... *Medecine/Sciences*, *32*(8–9), 771–773. https://doi.org/10.1051/medsci/20163208027

Aliste, A. J., Vieira, F. F., & Del Mastro, N. L. (2000). Radiation effects on agar alginates and carrageenan to beused as food additives.

Asasutjarit, R., Theerachayanan, T., Kewsuwan, P., Veeranondha, S., Fuongfuchat, A., & Ritthidej, G. C. (2017). Gamma sterilization of diclofenac sodium loaded- N-trimethyl chitosan nanoparticles for ophthalmic use. *Carbohydrate Polymers*, *157*, 603–612. https://doi.org/10.1016/j.carbpol.2016.10.029

Bushkalova, R., Farno, M., Tenailleau, C., Duployer, B., Cussac, D., Parini, A., … Girod Fullana, S. (2019). Alginate-chitosan PEC scaffolds: A useful tool for soft tissues cell therapy. *International Journal of Pharmaceutics*, *571*(August), 118692. https://doi.org/10.1016/j.ijpharm.2019.118692

Catoira, M. C., Fusaro, L., Di Francesco, D., Ramella, M., & Boccafoschi, F. (2019). Overview of natural hydrogels for regenerative medicine applications. *Journal of Materials Science: Materials in Medicine*, *30*(10). https://doi.org/10.1007/s10856-019-6318-7

Ceccaldi, C., Bushkalova, R., Alfarano, C., Lairez, O., Calise, D., Bourin, P., … Fullana, S. G. (2014). Evaluation of polyelectrolyte complex-based scaffolds for mesenchymal stem cell therapy in cardiac ischemia treatment. *Acta Biomaterialia*, *10*, 901–911. https://doi.org/10.1016/j.actbio.2013.10.027

Chalise, P. R., Hotta, E., Matak, K. E., & Jaczynski, J. (2007). Inactivation kinetics of Escherichia coli by pulsed electron beam. *Journal of Food Science*, *72*(7). https://doi.org/10.1111/j.1750-3841.2007.00451.x

Chmielewski, A. G., Migdal, W., Swietoslawski, J., Swietoslawski, J., Jakubaszek, U., & Tarnowski, T. (2007). Chemical-radiation degradation of natural oligoamino-polysaccharides for agricultural application. *Radiation Physics and Chemistry*, *76*(11–12), 1840–1842. https://doi.org/10.1016/j.radphyschem.2007.04.013

Ciesla, K. A. (2017). Radiation Modification of Polysaccharides and Their Composites / Nanocomposites. *Applications of Ionizing Radiation in Materials Processing*.

Croisier, F., & Jérôme, C. (2013). Chitosan-based biomaterials for tissue engineering. *European Polymer Journal*, *49*(4), 780–792. https://doi.org/10.1016/j.eurpolymj.2012.12.009

Daemi, H., & Barikani, M. (2012). Sharif University of Technology Synthesis and characterization of calcium alginate nanoparticles , sodium homopolymannuronate salt and its calcium nanoparticles. *Scientia Iranica*, *19*(6), 2023–2028. https://doi.org/10.1016/j.scient.2012.10.005

Deka, C., Deka, D., Moni, M., Kumar, D., & Kumar, D. (2016). Journal of Drug Delivery Science and Technology Synthesis of peppermint oil-loaded chitosan / alginate polyelectrolyte complexes and study of their antibacterial activity. *Journal of Drug Delivery Science and Technology*, *35*, 314–322. https://doi.org/10.1016/j.jddst.2016.08.007

Del Mastro, N. L. (2016). Radiation Influence on Edible Materials. In *Intech* (Vol. i, p. 13). https://doi.org/http://dx.doi.org/10.5772/57353

617 Ershov. (1987). Radiation-chemical transformation of chitosan.
618 Farag Zaied, S., Mohamed Youssef, B., Desouky, O., & Salah El Dien, M. (2007). Decontamination
619 of gum arabic with γ-rays or electron beams and effects of these treatments on the material.
620 *Applied Radiation and Isotopes*, *65*(1), 26–31. https://doi.org/10.1016/j.apradiso.2006.05.008
621 Feng, T., Du, Y., Li, J., Hu, Y., & Kennedy, J. F. (2008). Enhancement of antioxidant activity of
622 chitosan by irradiation, *73*, 126–132. https://doi.org/10.1016/j.carbpol.2007.11.003
623 Florczyk, S. J., Leung, M., Li, Z., Huang, J. I., Hopper, R. A., & Zhang, M. (2013). Evaluation of
624 three-dimensional porous chitosan – alginate scaffolds in rat calvarial defects for bone
625 regeneration applications. *Journal of Biomaterial Research*. https://doi.org/10.1002/jbm.a.34593
626 França, R., Mbeh, D. A., Samani, T. D., Le tien, C., Mateescu, M. A., Yahia, L., & Sacher, E. (2013).
627 The effect of ethylene oxide sterilization on the surface chemistry and in vitro cytotoxicity of
628 several kinds of chitosan, 1444–1455. https://doi.org/10.1002/jbmb.32964
629 Galante, R., Pinto, T. J. A., & Serro, A. P. (2017). Review Article Sterilization of hydrogels for
630 biomedical applications : A review rio Colac, 1–21. https://doi.org/10.1002/jbm.b.34048
631 Gómez, S., Vlad, M. D., López, J., & Fernández, E. (2016). Design and properties of 3D scaffolds for
632 bone tissue engineering. *Acta Biomaterialia*, *42*, 341–350.
633 https://doi.org/10.1016/j.actbio.2016.06.032
634 Gotzmann, G., Portillo, J., Wronski, S., Kohl, Y., Gorjup, E., Schuck, H., … Wetzel, C. (2018). Low-
635 energy electron-beam treatment as alternative for on-site sterilization of highly functionalized
636 medical products – A feasibility study. *Radiation Physics and Chemistry*, *150*(March), 9–19.
637 https://doi.org/10.1016/j.radphyschem.2018.04.008
638 Gryczka, U., Dondi, D., Chmielewski, A. G., Migdal, W., Buttafava, A., & Faucitano, A. (2009). The
639 mechanism of chitosan degradation by gamma and e-beam irradiation. *Radiation Physics and*
640 *Chemistry*, *78*(7–8), 543–548. https://doi.org/10.1016/j.radphyschem.2009.03.081
641 Gueven, O. (2004). An overview of current developments in applied radiation chemistry of polymers.
642 *Advances in Radiation Chemistry of Polymers, IAEA-TECDOC-1420*, (November), 33–39.
643 Guimarães, C. F., Gasperini, L., Marques, A. P., & Reis, R. L. (2020). The stiffness of living tissues
644 and its implications for tissue engineering. *Nature Reviews Materials*.
645 https://doi.org/10.1038/s41578-019-0169-1
646 Hartman, A. W., Nesbitt, R. U., Smith, F. M., & Nuessle, N. O. (1975). Viscosities of Acacia and
647 Sodium Alginate after sterilization by Cobalt-60. *Journal of Pharmaceutical Sciences*.
648 Helt-Hansen, J., Miller, A., Sharpe, P., Laurell, B., Weiss, D., & Pageau, G. (2010). Dμ-A new
649 concept in industrial low-energy electron dosimetry. *Radiation Physics and Chemistry*, *79*(1),
650 66–74. https://doi.org/10.1016/j.radphyschem.2009.09.002
651 Heux, L., Brugnerotto, J., Desbrières, J., Versali, M. F., & Rinaudo, M. (2000). Solid state NMR for
652 determination of degree of acetylation of chitin and chitosan. *Biomacromolecules*, *1*(4), 746–751.
653 https://doi.org/10.1021/bm000070y
654 Hien, N. Q., Nagasawa, N., Tham, L. X., Yoshii, F., Dang, V. H., Mitomo, H., … Kume, T. (2000).
655 Growth-promotion of plants with depolymerized alginates by irradiation. *Radiation Physics and*
656 *Chemistry*, *59*(1), 97–101. https://doi.org/10.1016/S0969-806X(99)00522-8
657 Hu, T., Yang, Y., Tan, L., Yin, T., Wang, Y., & Wang, G. (2014). Effects of gamma irradiation and
658 moist heat for sterilization on sodium alginate. *Bio-Medical Materials and Engineering*, *24*(5),
659 1837–1849. https://doi.org/10.3233/BME-140994
660 Ji, C., & Shi, J. (2013). Thermal-crosslinked porous chitosan scaffolds for soft tissue engineering
661 applications. *Materials Science & Engineering C*, *33*(7), 3780–3785.
662 https://doi.org/10.1016/j.msec.2013.05.010
663 Jose, G., Shalumon, K. T., & Chen, J.-P. (2019). Natural Polymers Based Hydrogels for Cell Culture
664 Applications. *Current Medicinal Chemistry*, *27*(16), 2734–2776.
665 https://doi.org/10.2174/0929867326666190903113004
666 Kume, T., Nagasawa, N., & Yoshii, F. (2002). Utilization of carbohydrates by radiation processing.
667 *Radiation Physics and Chemistry*, *63*(3–6), 625–627. https://doi.org/10.1016/S0969-
668 806X(01)00558-8
669 Kuznetsova, T. A., Andryukov, B. G., Besednova, N. N., Zaporozhets, T. S., & Kalinin, A. V. (2020).
670 Marine Algae Polysaccharides as Basis for Wound Dressings , Drug Delivery , and Tissue
671 Engineering : A Review. *Journal of Marine Science and Engineering*.

672 Lamarche, C. (2019). *Compréhension de l'efficacité bactéricide de différentes technologies de haute*
673 *puissance pulsée.*
674 Lamarche, C., & Demol, G. (2018). *Bacteria inactivation by pulsed electron beam.*
675 Lambert, B., & Martin, J. (2013). Sterilization of Implants and Devices. In *Biomaterials Science: An*
676 *Introduction to Materials: Third Edition* (Third Edit, pp. 1339–1353). Elsevier.
677 https://doi.org/10.1016/B978-0-08-087780-8.00125-X
678 Lawrie, G., Keen, I., Drew, B., Chandler-Temple, A., Rintoul, L., Fredericks, P., & Grøndahl, L.
679 (2007). Interactions between alginate and chitosan biopolymers characterized using FTIR and
680 XPS. *Biomacromolecules*, *8*(8), 2533–2541. https://doi.org/10.1021/bm070014y
681 Lee, K. Y., & Mooney, D. J. (2012). Alginate: Properties and biomedical applications. *Progress in*
682 *Polymer Science (Oxford)*, *37*(1), 106–126. https://doi.org/10.1016/j.progpolymsci.2011.06.003
683 Leo, W. J., Mcloughlin, A. J., & Malone, D. M. (1990). Effects of Sterilization Treatments on Some
684 Properties of Alginate Solutions and Gels. *Biotechnology Progress*, *6*(1), 51–53.
685 https://doi.org/10.1021/bp00001a008
686 Li, Z., Ramay, H. R., Hauch, K. D., Xiao, D., & Zhang, M. (2005). Chitosan-alginate hybrid scaffolds
687 for bone tissue engineering. *Biomaterials*, *26*(18), 3919–3928.
688 https://doi.org/10.1016/j.biomaterials.2004.09.062
689 Lim, L. Y., Khor, E., & Koo, O. (1998). Irradiation of chitosan. *Journal of Biomedical Materials*
690 *Research*, *43*(3), 282–290. https://doi.org/10.1002/(SICI)1097-4636(199823)43:3<282::AID-
691 JBM9>3.0.CO;2-J
692 Luo, Y., & Wang, Q. (2014). Recent development of chitosan-based polyelectrolyte complexes with
693 natural polysaccharides for drug delivery. *International Journal of Biological Macromolecules*,
694 *64*, 353–367. https://doi.org/10.1016/J.IJBIOMAC.2013.12.017
695 Mäder, K., Domb, A., & Swartz, H. M. (1996). Gamma-sterilization-induced radicals in biodegradable
696 drug delivery systems. *Applied Radiation and Isotopes*, *47*(11–12), 1669–1674.
697 https://doi.org/10.1016/S0969-8043(96)00236-9
698 Matsuhashi, S., & Kume, T. (1997). Enhancement of Antimicrobial Activit y of Chitosan b y
699 Irradiation, *00*, 1–5.
700 Meka, V. S., Sing, M. K. G., Pichika, M. R., Nali, S. R., Kolapalli, V. R. M., & Kesharwani, P.
701 (2017). A comprehensive review on polyelectrolyte complexes. *Drug Discovery Today*, *22*(11),
702 1697–1706. https://doi.org/10.1016/j.drudis.2017.06.008
703 Mendes, Brandão, & Da Silva. (2004). Ethylene oxide sterilization of medical devices: A review.
704 https://doi.org/10.1016/j.ajic.2006.10.014
705 Munarin, F., Bozzini, S., Visai, L., Tanzi, M. C., & Petrini, P. (2013). Sterilization treatments on
706 polysaccharides: Effects and side effects on pectin. *Food Hydrocolloids*, *31*, 74–84.
707 https://doi.org/10.1016/j.foodhyd.2012.09.017
708 Nagasawa, N., Mitomo, H., Yoshii, F., & Kume, T. (2000). Radiation-induced degradation of sodium
709 alginate. *Polymer Degradation and Stability*, *69*(3), 279–285. https://doi.org/10.1016/S0141-
710 3910(00)00070-7
711 NF EN ISO 11137-2. 11137-2, 2006 61010-1 © Iec:2001 § (2006).
712 Pawlak, A., & Mucha, M. (2003). Thermogravimetric and FTIR studies of chitosan blends, *396*, 153–
713 166.
714 Pennesi, G., Scaglione, S., Giannoni, P., & Quarto, R. (2011). Regulatory Influence of Scaffolds on
715 Cell Behavior: How Cells Decode Biomaterials. *Current Pharmaceutical Biotechnology*, *12*(2),
716 151–159. https://doi.org/10.2174/138920111794295684
717 Ph. Eur. 2.6.1. (2008). *2.6. biological tests*.
718 Rao, S. B., & Sharma, C. P. (1995). Sterilization of Chitosan Implications. *Journal of Biomaterials*
719 *Applications*, *10*.
720 Reed, S., & Wu, B. M. (2015). Biological and mechanical characterization of chitosan-alginate
721 scaffolds for growth factor delivery and chondrogenesis, *2*, 272–282.
722 https://doi.org/10.1002/jbm.b.33544
723 Rosiak, J., Ulanski, P., Kucharska, M., Dutkiewicz, J., & Judkiewizc, L. (1992). Radiation sterilization
724 of chitosan sealant for vascular prostheses. *Journal of Radioanalytical and Nuclear Chemistry*.
725 Sæther, H. V., Holme, H. K., Maurstad, G., Smidsrød, O., & Stokke, B. T. (2008). Polyelectrolyte
726 complex formation using alginate and chitosan. *Carbohydrate Polymers*, *74*(4), 813–821.

https://doi.org/10.1016/j.carbpol.2008.04.048
San Juan, A., Montembault, A., Gillet, D., Say, J. P., Rouif, S., Bouet, T., … David, L. (2012). Degradation of chitosan-based materials after different sterilization treatments. *IOP Conference Series: Materials Science and Engineering*, *31*, 2–7. https://doi.org/10.1088/1757-899X/31/1/012007
Santos, E., Hernández, R. M., Pedraz, J. L., & Orive, G. (2012). Novel advances in the design of three-dimensional bio-scaffolds to control cell fate: Translation from 2D to 3D. *Trends in Biotechnology*, *30*(6), 331–341. https://doi.org/10.1016/j.tibtech.2012.03.005
Sartori, C., Finch, D. S., & Ralph, B. (1997). D e t e r m i n a t i o n of the cation content of alginate thin films by, *38*(1), 43–51.
Sen, M., & Atik, H. (2012). The antioxidant properties of oligo sodium alginates prepared by radiation-induced degradation in aqueous and hydrogen peroxide solutions. *Radiation Physics and Chemistry*, *81*, 816–822. https://doi.org/10.1016/j.radphyschem.2012.03.025
Sen, M., Rendevski, S., Akkas-Kavaklı, P., & Sepehrianazar, A. (2010). Effect of G/M ratio on the radiation-induced degradation of sodium alginate. *Radiation Physics and Chemistry*, *79*, 279–282. https://doi.org/10.1016/j.radphyschem.2009.08.028
Shelke, N. B., James, R., Laurencin, C. T., & Kumbar, S. G. (2014). Polysaccharide biomaterials for drug delivery and regenerative engineering. *Polymers for Advanced Technologies*, *25*(5), 448–460. https://doi.org/10.1002/pat.3266
Silindir, M., & Özer, A. Y. (2009). Sterilization methods and the comparison of E-beam sterilization with gamma radiation sterilization. *Fabad Journal of Pharmaceutical Sciences*, *34*(1), 43–53.
Silva, R. M., Elvira, C., Mano, J. F., Roma, J. S. A. N., & Reis, R. L. (2004). Influence of beta radiation sterilisation in properties of new chitosan / soybean protein isolate membranes for guided bone regeneration, *5*, 523–528.
Stoppel, W. L., White, J. C., Horava, S. D., Henry, A. C., Roberts, S. C., & Bhatia, S. R. (2013). Terminal sterilization of alginate hydrogels : Efficacy and impact on mechanical properties, 877–884. https://doi.org/10.1002/jbm.b.33070
Stößel, M., Metzen, J., Wildhagen, V. M., Helmecke, O., Rehra, L., Freier, T., & Haastert-talini, K. (2018). Long-Term In Vivo Evaluation of Chitosan Nerve Guide Properties with respect to Two Different Sterilization Methods, *2018*.
Sun, J., & Tan, H. (2013). Alginate-Based Biomaterials for Regenerative Medicine Applications, 1285–1309. https://doi.org/10.3390/ma6041285
Sun, W., Chen, G., Wang, F., Qin, Y., Wang, Z., Nie, J., & Ma, G. (2018). Polyelectrolyte-complex multilayer membrane with gradient porous structure based on natural polymers for wound care. *Carbohydrate Polymers*, *181*(October 2017), 183–190. https://doi.org/10.1016/j.carbpol.2017.10.068
Tallentire, A., Miller, A., & Helt-hansen, J. (2010). A comparison of the microbicidal effectiveness of gamma rays and high and low energy electron radiations. *Radiation Physics and Chemistry*, *79*(6), 701–704. https://doi.org/10.1016/j.radphyschem.2010.01.010
Taskin, P., Canisag, H., & Sen, M. (2014). The effect of degree of deacetylation on the radiation induced degradation of chitosan. *Radiation Physics and Chemistry*, *94*, 236–239. https://doi.org/10.1016/j.radphyschem.2013.04.007
Thevarajah, J. J., Bulanadi, J. C., Wagner, M., Gaborieau, M., & Castignolles, P. (2016). Towards a less biased dissolution of chitosan. *Analytica Chimica Acta*, *935*, 258–268. https://doi.org/10.1016/j.aca.2016.06.021
Vandenbossche, G. M. R. (1993). Influence of the sterilization process on alginate dispersions, 22–24.
Vilén, E. M., Klinger, M., & Sandström, C. (2011). Application of diffusion-edited NMR spectroscopy for selective suppression of water signal in the determination of monomer composition in alginates. *Magnetic Resonance in Chemistry*, *49*(9), 584–591. https://doi.org/10.1002/mrc.2789
Wang, L., Khor, E., Wee, A., & Lim, L. Y. (2002). Chitosan-alginate PEC membrane as a wound dressing: Assessment of incisional wound healing. *Journal of Biomedical Materials Research*, *63*(5), 610–618. https://doi.org/10.1002/jbm.10382
Wasikiewicz, J. M., Yoshii, F., Nagasawa, N., Wach, R. A., & Mitomo, H. (2005). Degradation of chitosan and sodium alginate by gamma radiation, sonochemical and ultraviolet methods.

Radiation Physics and Chemistry, *73*, 287–295. https://doi.org/10.1016/j.radphyschem.2004.09.021

Wenwei, Z., Xiaoguang, Z., Li, Y., Yuefang, Z., & Jiazhen, S. (1993). Some chemical changes in chitosan induced by γ-ray irradiation. *Polymer Degradation and Stability*, *41*(1), 83–84. https://doi.org/10.1016/0141-3910(93)90065-Q

Xu, Y., Xia, D., Han, J., Yuan, S., Lin, H., & Zhao, C. (2017). Design and fabrication of porous chitosan scaffolds with tunable structures and mechanical properties. *Carbohydrate Polymers*, *177*(August), 210–216. https://doi.org/10.1016/j.carbpol.2017.08.069

Yanagisawa, M., Kato, Y., Yoshida, Y., & Isogai, A. (2006). SEC-MALS study on aggregates of chitosan molecules in aqueous solvents : Influence of residual N -acetyl groups, *66*, 192–198. https://doi.org/10.1016/j.carbpol.2006.03.008

Yoksan, R., Akashi, M., Miyata, M., & Chirachanchai, S. (2004). Optimal γ-ray dose and irradiation conditions for producing low-molecular-weight chitosan that retains its chemical structure. *Radiation Research*, *161*(4), 471–480. https://doi.org/10.1667/RR3125

Yu, H., Cauchois, G., Schmitt, J., Louvet, N., & Six, J. (2017). Is there a cause-and-e ff ect relationship between physicochemical properties and cell behavior of alginate-based hydrogel obtained after sterilization ? *Journal of the Mechanical Behavior of Biomedical Materials*. https://doi.org/10.1016/j.jmbbm.2017.01.038

Zainol, I., Akil, H. M., & Mastor, A. (2009). Effect of γ-irradiation on the physical and mechanical properties of chitosan powder. *Materials Science and Engineering C*, *29*(1), 292–297. https://doi.org/10.1016/j.msec.2008.06.026

Zhu, H., Xu, J., Li, S., Sun, X., Yao, S., & Wang, S. (2008). Effects of high-energy-pulse-electron beam radiation on biomacromolecules. *Science in China, Series B: Chemistry*, *51*(1), 86–91. https://doi.org/10.1007/s11426-008-0017-4

Ziaie, F., Anvari, F., Ghaffari, M., & Borhani, M. (2005). Dose rate effect on LDPE cross-linking induced by electron beam irradiation. *Nukleonika*, *50*(3), 125–127.